Simulation analysis method of drainage system of tideland paddy zone

Yong-Gun Kim[1], Kwang-Min Han[1,*], Kyungmin Hwang[2], Ji-Song Choe[1], Tong-Ho Ri[1], Gyong-Chol Pak[1], Hyon-Min Rim[1]

*Corresponding author: Kwang-Min Han

Email address: 15764500263@163.com

1 Department of Hydrology, Faculty of Global Environmental Science, **Kim Il Sung** University, Pyongyang, the Democratic People's Republic of Korea

2 University of Sciences, Pyongyang, Democratic People's Republic of Korea

Abstract

The tideland paddy zone drainage system plays an important role in preventing flood damage and protecting the tideland paddy zone by draining the rainwater from the paddy zones and the surrounding catchments in good time. Therefore, scientific design of drainage system and accurate assessment of drainage capacity in tideland paddy zones are important for sustainable development in agricultural production and safe farming.

So far, many theories and methods have been proposed for drainage systems and many programs have been developed to design urban drainage systems, river systems, and simulate and analyze their drainage and pumping capacities, such as SWMM, HEC, and DHI, but have the drawbacks that it is impossible to simulate and analyze the flood runoff process in drainage systems with complex combined structure of paddy fields and drainage channels.

This paper presents an efficient method of drainage system numerical analysis method of a tideland paddy zone. This method combines a flow simulation model in drainage canals based on one-dimensional unsteady flow numerical method and a runoff analysis model in a paddy zone where many paddy fields are connected differently. By applying this method, a drainage system analysis program of tideland paddy zone was developed. The program comprehensively analyzed and evaluated the drainage capacity of the Suk Hwa tideland drainage system in the DPRK and verified its accuracy and effectiveness.

Keywords Drainage system; Drainage canal; Paddy; Tideland; Flood control

Introduction

A drainage system of tideland is a system of hydraulic structures consisting of drainage channels, drainage gates and regulating pond that are installed to prevent flood damage by controlling runoff flow and flow direction of rainwater. Generally, drainage systems differ in their mission and method of installation depending on the hydrological characteristics and location of the area to be installed.

So far, various kinds of programs related to water resources management and water flow numerical analysis have been used for drainage system simulation analysis in different parts of the world.

Typical of these programs are SWMM (Storm Water Management), HEC (Hydrological Engineering Center), DHI (Danish Hydraulic Institute), SOBEK and SWAT (Christou et al. 2017, Ontowirijo et al. 2023, Rujner et al. 2018, Patra et al. 2016, Dau et al. 2017, Gerlach et al. 2016).

The SWMM model was first developed in 1971 and has been widely applied in a number of urban areas with several updates, and has been applied to non-urban areas. In the SWMM model, one basin is generally divided into several sub-catchments, based on the characteristics of each sub-catchment, its runoff process is calculated separately, and synthesizes the runoff of each sub-catchment along the sewer network.

Harsha et al. (2020) used the SWMM model to evaluate drainage capacity in large cities in India and Shanghai City in China and to evaluate the accuracy. In this study, the computational results of the SWMM model are shown to be relatively ideal and reliable.

Some researchers have proposed a method for estimating drainage capacity of urban drainage networks by combining GIS and SWMM models (Jiang et al. 2015; Perin et al. 2020). The paper establishes a geospatial information database design and modeling parameter auto-determination method for automatic determination of modeling parameters, problems arising in modeling the storm network using SWMM model, and evaluates the existing storm network drainage capacity of the study area. Tu et al. (2020) also performed rainfall runoff simulations in several large cities around the world, using the same approach as S. Sri Harsha et al. (2020).

Khodashenas et al. (2016) performed simulations and evaluations of urban drainage systems in the city using SWMM models and GIS. GIS was used for extraction of attribute information, parameter setting and calibration for catchments, and SWMM model was used for rainfall runoff simulation of urban drainage system.

Pachaly et al. (2020) designed an efficient drainage system in a city of India by combining SWMM model with MIKE URBAN model. The SWMM model is one-dimensional and cannot be used to simulate flood extent or flooding depth. Therefore, a two-dimensional MIKE URBAN model was used to overcome the limitations of the SWMM model. The SWMM model shows the flood at the nodes, and the MIKE URBAN model shows the flood extent, the flooding depth and the direction of the surface flow over the surface.

The SWMM model is suitable for urban areas with relatively complex hydro-hydraulic conditions, and it has the advantages that the simple model structure makes it easy to design drainage systems, easy to understand and run time short, but because of not assuming flow interactions between sub-catchments, it has the disadvantages of oversimplifying surface runoff. Hence, it is not possible to simulate rainfall runoff in tideland drainage systems where the sub-catchments, such as paddy fields, are interconnected and interact.

The SOBEK model is a fully coupled hydraulic model capable of simulation of drainage channel and surface runoff developed in the Netherlands. SOBEK includes rainfall runoff module and water quality module.

Carrivick (2006) proposed a method to redesign the drainage system of a flooded area due to large scale rainfall using the SOBEK model. In addition, several researchers have used the SOBEK model to design drainage system and evaluate drainage capacity in large-scale floodplains (Happonen et al. 2016; Rahman et al. 2014; Afrasiabikia et al. 2017; Tarekegn et al. 2010). The SOBEK model is very efficient in estimating the drainage capacity in areas with high rainfall and large catchment area. However, this model also cannot simulate the flow dynamics in paddy fields and drainage systems interacting with each other through the irrigation gate.

The program for the simulation analysis of agricultural land drainage system includes the SWAT model.

The SWAT model is a continuous, physically-based, semi-distributed watershed model that was originally developed by the USDA Agricultural Research Service to assess the impact of agricultural land use management practices on water, sediment, and nutrient yields in large basins with different soil types, land uses, and management practices.

The SWAT model divides a watershed into a number of sub-basins connected by stream networks. Each sub-basin is further divided into a number of hydrologic response units (HRUs) that are unique combinations of different land uses, soils, and surface slopes.

Some researchers used the SWAT model to evaluate the drainage capacity of a watershed with and without the introduction of subsurface drainage system (Addab et al. 2022, Chen et al. 2022). In these studies, a new drainage algorithm was proposed to estimate drainage capacity and four parameters were selected for groundwater runoff assessment: impervious layer depth, subsurface drainage depth, drainage time for paddy field capacity, and drainage delay. Subsurface drainage depth was determined by the depth of the drainage pipe and the remaining parameters were determined by comparing the simulated values for the drainage pipe flow with the observed values. Then, the simulations were performed for the period 2008-2010, and simulated hydrological elements were compared with and without the installation of the drainage pipe. The introduction of the subsurface drainage system resulted in a reduction in mean surface runoff by about 30% and mean soil water content by about 10%, while subsurface drainage discharge accounted for about 16% of annual rainfall and about 37% of the total catchment runoff.

Many researchers have used SWAT models to simulate the effects of subsurface drainage on river discharge in large catchments (Roy et al. 2021, Hoghooghil 2021, KhornN et al. 2022, Nasiri et al. 2020, Beharry et al. 2021, Xie et al. 2023). The SWAT model is suitable for simulating and analyzing the subsurface drainage system because it provides a relatively accurate estimate of long-term subsurface drainage discharge and sediment discharge in large-scale catchments. However, since the subsurface drainage system is simulated and analyzed mainly, it has the disadvantage that it is not applicable in areas without subsurface drainage systems.

Hence, this paper presents a paddy zone drainage system simulation analysis method that combines a flow simulation analysis method in paddy zone with different combinations of various scale paddy fields and flow simulation analysis in drainages network based on one-dimensional unsteady flow numerical method. The runoff simulation analysis method of paddy zone consists of a method for calculating runoff through the irrigation gates in individual paddy fields and a rank search algorithm for paddy fields with complex coupling. The flow simulation analysis method in a drainage network consists of the numerical calculation of water flow in a single channel, the internal boundary treatment method at the junction of paddy field and the channel, and the internal boundary treatment method in the case of a drain at the lower boundary of the channel. The simulation analysis method of the paddy zone drainage system was applied to the calculation of the drainage capacity of the Suk Hwa tideland drainage system in Sonchon County, North Phyongan Province of the DPRK, and its accuracy and effectiveness were verified.

Methods

Analysis of runoff simulation in paddy zone

Models of paddy zone runoff simulation

In paddy zones, rainwater enters drainage via interconnected irrigation gate, unlike in dry fields or hill-slopes.

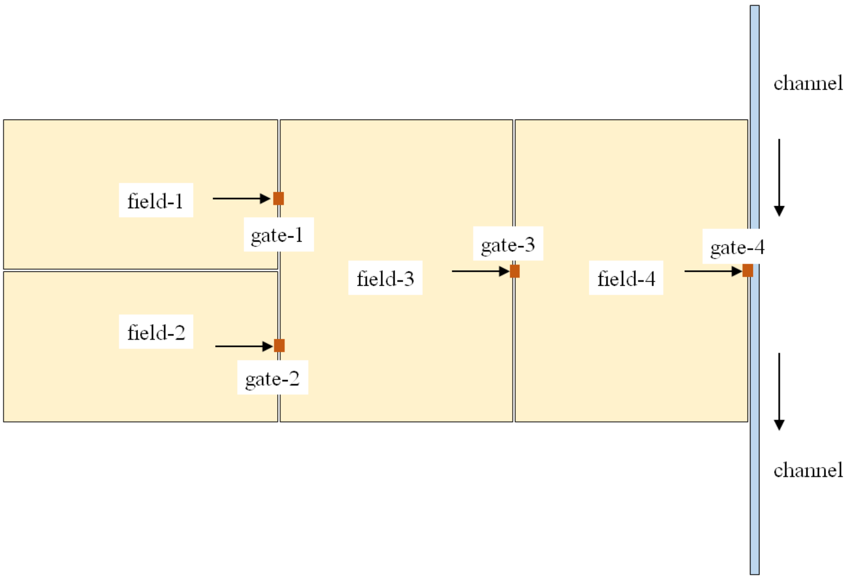

Fig. 1. Division of paddy field for numerical modeling

To numerically model the paddy field discharge, consider paddy fields connected to a drainage channel as shown in Fig. 1. As shown in the figure, paddy field-1 and paddy field-2 are connected side by side with paddy field-3 and paddy field-3 is connected with paddy field-4.

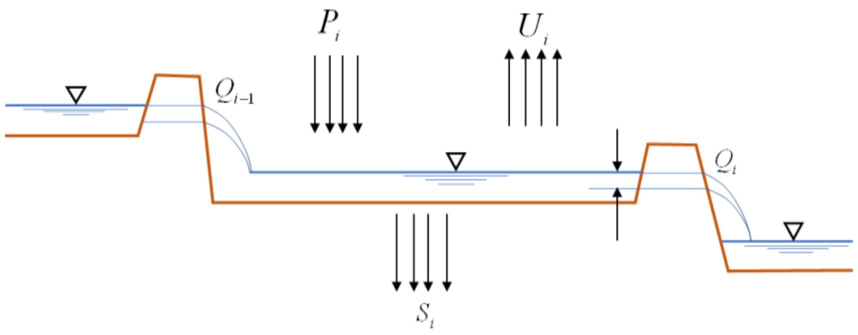

Fig.2. Runoff of the case when the irrigation gate is not flooded

When rainwater runs down in the paddy zone, the water balance relationship is shown in Fig. 2 when the irrigation gate in the i[th] paddy field is not flooded.

When the irrigation gate is flooded, there are cases where the paddy field is connected to a drainage channel and to a paddy field (Fig. 3).

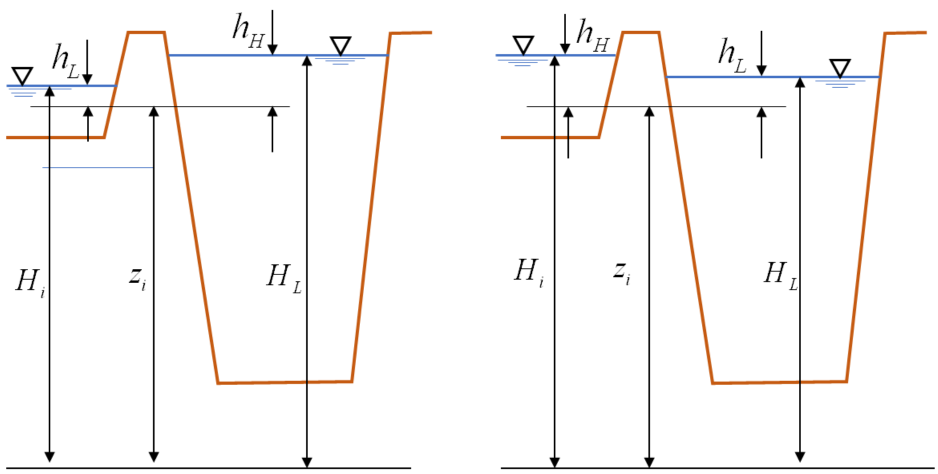

Fig. 3. Runoff of the case when the irrigation gate is flooded

The model of the runoff simulation, which reflects the water balance relationship between individual paddy fields shown in Figs. 2 and 3, can be written as follows:

$$\begin{cases} w_i \dfrac{dh_i(t,L)}{dt} = q_i(t,E) - Q_i(t,C) + w_i P_i(t) + \Delta W_i(t) \\ \Delta W_i(t) = -U_i(t) - S_i(t) \end{cases} \tag{1}$$

Where, i-paddy field number, $P_i(t)$-precipitation of paddy field (m), $\Delta W_i(t)$-sum of deviations of other water balance components of paddy field (m^3), $U_i(t)$-evaporation of paddy field (m^3), $S_i(t)$-Infiltraion of paddy field (m^3), w_i-the area of paddy field (m^2).

The depth of water (m) above the irrigation gate of paddy field $h_i(t,L)$ is expressed according to the combined conditions of paddy field and drainage as follows:

$$h_i(t,L) = \begin{cases} H_i(t) - z_i, & (L=0) \\ H_i(t) - H_{\mathrm{L}}(t), & (L=1) \\ H_i(t) - H_{i+1}(t), & (L=2) \end{cases} \tag{2}$$

Where, i-paddy field number, $H_i(t)$-water level height of paddy field(m), z_i-irrigation gate height of the paddy field (m), $H_L(t)$-water level height of the drainage channel (m), L={0,1,2}, L=0: irrigation gate is not flooded, L=1: irrigation gate is flooded and is connected to the drainage channel; L=2: irrigation gate is flooded and is connected to the paddy field.

$q_i(t,E)$ is the amount of water inflow into the paddy field (m^3/s), is expressed as follows:

$$q_i(t,E)=\begin{cases}0, & (E=0)\\ \sum_{j=1}^{l} Q_{i-1,j}(t), & (E=1)\end{cases} \tag{3}$$

Where, E={0,1}, E=0: without paddy field influx; E=1: with paddy field influx, l- number of paddy fields influx into the paddy field, $Q_{i-1,j}(t)$-discharge of irrigation gate in j^{th} paddy field influx into the i^{th} paddy field (m^3/s).

$Q_i(t,C)$ is the discharge from the paddy field (m^3/s) and is expressed as follows:

$$Q_i(t,C)=\begin{cases}\sum_{j=1}^{l} Q_{ij}(t) & (C=0)\\ Q_i(t), & (C=1)\end{cases} \tag{4}$$

Where, C={0,1}, C=0: the case of flow from paddy field to paddy field, and C=1: the case of flow from paddy field to drainage.

$Q_i(t)$ is the discharge through the paddy field irrigation gate, is given by

$$Q_i(t)=\begin{cases}m_i\sqrt{2g}B_i\left(h_i(t,L)\right)^{3/2}, & (L=0)\\ m_i'\sqrt{2g}B_ih_i'\dfrac{h_i(t,L)}{\sqrt{|h_i(t,L)|}}, & (L=1,2)\end{cases} \tag{5}$$

Where, L={0,1,2}, L=0: irrigation gate is not flooded, L=1: irrigation gate is flooded and is connected to the drainage channel; L=2: irrigation gate is flooded and is connected to the paddy field, B_i-width of paddy field irrigation gate (m), g-acceleration of gravity (m^2/s), and $h_i(t,L)$ is calculated by Eq. (3). The m_i is the discharge coefficient of the paddy field irrigation gate, and m'_i is the discharge coefficient of the flooded irrigation gate.

By the equations considered above, a system of main equations for the simulation modeling of paddy zone runoff is constructed.

Numerical modeling of individual paddy field runoff

Given rainfall in paddy fields, other water balance components such as evaporation, infiltration, or neglecting minor amounts, the main unknowns in Eq. (1) are $h_i(t,L)$ and $Q_i(t)$.

From the Eq. (1), the continuity equation for the i^{th} paddy field is given by

$$w_i\frac{dh_i(t,L)}{dt}=P(t)w_i-Q_i(t,C) \tag{6}$$

This can be expressed in a finite difference way as follows:

$$w_i\frac{H_{i,n+1}-H_{i,n}}{\Delta t}=w_iP_n-\frac{Q_{i,n+1}+Q_{i,n}}{2} \tag{7}$$

Where, i-paddy field number, n-time number, w_i -area of the paddy field. $H_{i,n}$, $H_{i,n+1}$-paddy field surface water level, and P_n-the rain intensity, $Q_{i,n}$, $Q_{i,n+1}$-The flow rate of the paddy field irrigation gate.

From this equation, the flow rate is obtained as follows:

$$Q_{i,n+1}=-\frac{2w_i}{\Delta t}H_{i,n+1}+\frac{2w_i}{\Delta t}H_{i,n}-Q_{i,n}+2w_iP_n \tag{8}$$

The values of $Q_{i,n+1}$, $H_{i,n+1}$ in the i^{th} paddy field are calculated using the well-known Newton's iteration method, in which case the following equations are used, depending on the two cases when the irrigation gate is not flooded and when it is flooded.

Runoff when the irrigation gate is not flooded

$$\begin{cases} Q_{i,K+1} = Q_{i,K} + \left(\dfrac{dQ_i}{dh_i}\right)_K \cdot \Delta h \\ \Delta h_i = H_{i,K+1} - H_{i,K} \\ D = \left(\dfrac{dQ_i}{dh_i}\right)_K = \dfrac{3}{2} m_i \sqrt{2g} B_i h_{i,K}^{1/2} \\ H_{i,K+1} = \left[\dfrac{D}{3}(H_{i,K} + 2z_i) + 2w_i P_n + \dfrac{2w_i}{\Delta t} H_{i,n} - Q_{i,n}\right] / \left(\dfrac{2w_i}{\Delta t} + D\right) \end{cases} \tag{9}$$

Where, m_i-the discharge coefficient of the paddy field irrigation gate, g-acceleration of gravity (m^2/s), B_i-width of paddy field irrigation gate (m), h_i=H_i-z_i, z_i-irrigation gate height of the paddy field, $Q_{i,K+1}$-the K+1th approximation of Q_i, and $H_{i,K+1}$-the K+1th approximation of H_i.

Runoff when the irrigation gate is flooded

When the irrigation gate is flooded, there are cases where the water level of the paddy field is higher than the drainage channel and lower.

Considering both cases, $H_{i,k+1}$ is calculated using the following equation :

$$b_i H_{i,K+1} + f_i H_{L,K+1} = l_i \tag{10}$$

The coefficients are

$$b_i = \begin{cases} \dfrac{2w_i}{\Delta t} + D_{dif} & \left(H_{i,K+1} \geq H_{L,K+1}\right) \\ \dfrac{2w_i}{\Delta t} + D_{dif} + D_{low} & \left(H_{i,K+1} < H_{L,K+1}\right) \end{cases} \tag{11}$$

$$f_i = \begin{cases} D_{low} - D_{dif} & \left(H_{i,K+1} \geq H_{L,K+1}\right) \\ -D_{dif} & \left(H_{i,K+1} < H_{L,K+1}\right) \end{cases} \tag{12}$$

$$l_i = D_{dif}\left(H_{i,K} - H_{L,K}\right) + D_{low} z_i + \left(2w_i P_n + \frac{2w_i}{\Delta t} H_{i,n} - Q_{i,n}\right) \tag{13}$$

$$D_{low} = \left(\frac{\partial Q_i}{\partial h_{low}}\right)_K = \frac{m'_i \sqrt{2g} B_i \left(H_{i,K} - H_{L,K}\right)}{\sqrt{\left|H_{i,K} - H_{L,K}\right|}} \tag{14}$$

$$\Delta h_{low} = H_{low,K+1} - H_{low,K} \tag{15}$$

$$D_{dif} = \left(\frac{\partial Q_i}{\partial H_{dif}}\right)_K = \frac{m' \sqrt{2g} B_i \left(H_{low,K} - z_i\right)}{2\sqrt{\left|H_{i,K} - H_{L,K}\right|}} \tag{16}$$

$$\Delta h_{dif} = (H_{i,K+1} - H_{L,K+1}) - (H_{i,K} - H_{L,K}) \tag{17}$$

Where, the m'_i-the discharge coefficient of the flooded irrigation gate, and $H_{L,k+1}$-the K+1th approximation of drainage water level H_L.

As can be seen, to express the water depth in the paddy field H_i in the form of a linear equation, when the irrigation gate is not flooded, Eq. (9) can be used and when the irrigation gate is flooded, Eq. (10) can be used with the flow numerical calculation method in the drainage channel.

One-dimensional numerical modeling of unsteady flow processes in drainage system

In this paper, a one-dimensional numerical method for unsteady flow processes in a drainage system, where a large number of paddy fields are connected to each other and the channel is separated or merged together to form a complex structure is proposed.

Basic Equations of One-Dimensional Unsteady Flow in Drainage

The system of basic equations of one-dimensional unsteady flow in an open channel of drainage consists of the continuity equation and the equations of motion of the water flow [27].

$$\begin{cases} B\dfrac{\partial Z}{\partial t}+\dfrac{\partial Q}{\partial x}=q \\ \dfrac{\partial Q}{\partial t}+\dfrac{\partial}{\partial x}\left(\dfrac{Q^2}{A}\right)+gA\left(\dfrac{\partial Z}{\partial x}+\dfrac{Q|Q|}{k^2}\right)=0 \end{cases} \tag{18}$$

Where, x-spatial coordinates representing the stream-wise distance (m), A-water flow area (m^2), Q-cross-sectional average flow (m^3/s), and Z-water level (m).

$$k=\frac{1}{n}AR^{2/3}$$

Where, n is the bed roughness coefficient, R is the hydraulic radius (m).

Applying the Preissmann implicit difference scheme to Eq. (18) and after some linearization, the following numerical model is obtained.

$$\begin{cases} A_{1i}\Delta Q_i + B_{1i}\Delta Z_i + C_{1i}\Delta Q_{i+1} + D_{1i}\Delta Z_{i+1} = E_{1i} \\ A_{2i}\Delta Q_i + B_{2i}\Delta Z_i + C_{2i}\Delta Q_{i+1} + D_{2i}\Delta Z_{i+1} = E_{2i} \end{cases} \tag{19}$$

Where, A_{1i}~E_{1i}, A_{2i}~E_{2i} are coefficients determined by the water flow area A^n, water flow width B^n, discharge Q^n, and water heights of the previous stage.

Eq. (19) is solved by applying the backward-forward method. The forward transfer coefficients H_j, I_j, J_j, F_{j+1}, G_{j+1} are determined by the forward process and ΔQ_i, ΔZ_i are calculated by the backward process.

The method of calculating the backward-forward coefficient without internal boundary points has been described in detail in Kim et al. (2019).

Since the drainage system of paddy zones are connected to each other and one channel is connected to several paddy fields so that the drainage system are forming a complex internal structure in which the water flow is confluent with each other, the numerical calculation cannot be carried out by the method presented above alone, and the internal boundary treatment methods at these confluences must be combined. The internal boundary treatment methods for drainage systems include the treatment of confluences when the water flow of the paddy field enters in the drainage channel if the paddy irrigation gate is not flooded, the treatment of junctions when the water flow of the drainage channel enters in the paddy field, the treatment of channel sections when several drainage channel are combined and draining gate is installed in the outlet of drainage channel. The internal boundary treatment methods when several drainage channel are combined and draining gate is installed in the outlet of drainage channel has been described in detail in Kim et al. (2019). Hence, this paper only describes the internal boundary treatment when the water flow of paddy field enters in the drainage channel and the water flow of the drainage channel enters into the paddy field.

Internal boundary point treatment method at the location where paddy field water-flow enters the drainage channel

The case of a paddy field connected to the side of the drainage channel is shown in Fig. 4.

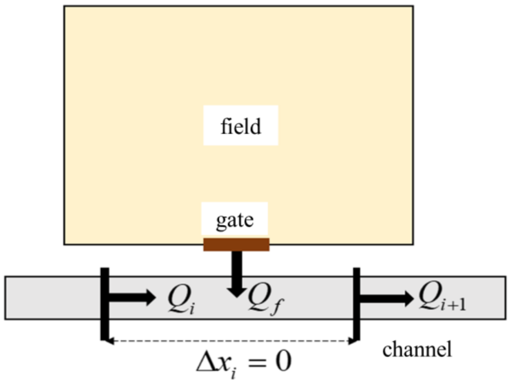

Fig.4. When the water flow of paddy field enters into the drainage channel

As shown in the figure, we set up one virtual channel interval. Then, the distance between the i^{th} section and $i+1^{th}$ section of the virtual channel interval is set to zero. The continuity condition of the flow between the two sections is established as follows.

$$\begin{cases} Z_i = Z_{i+1} \\ Q_i + Q_f = Q_{i+1} \end{cases} \tag{20}$$

Let us transform Eq. (20) into

$$Z_{i+1}^n + \Delta Z_{i+1} = Z_i^n + \Delta Z_i \tag{21}$$

$$Q_{i+1}^n + \Delta Q_{i+1} = Q_i^n + \Delta Q_i + Q_f \tag{22}$$

Ordering Eq. (21) into

$$\begin{cases} \Delta Q_{i+1} = \Delta Q_i + Q_i^n - Q_{i+1}^n + Q_f \\ \Delta Z_i = \Delta Z_{i+1} + \left(Z_{i+1}^n - Z_i^n \right) \end{cases} \tag{23}$$

Substituting the relationship of $\Delta Q_i = F_i \Delta Z_i + G_i$ into the first equation of Eq. (23) and ordering, after the model coefficients ΔZ_i and ΔQ_{i+1} are determined by the forward model coefficients H_i, I_i, J_i, F_{i+1}, G_{i+1} as follows:

$$\begin{cases} F_{i+1} = F_i \\ G_{i+1} = G_i + Q_i^n - Q_{i+1}^n + Q_f \\ H_i = 0 \\ I_i = 1 \\ J_i = Z_{i+1}^n - Z_i^m \end{cases} \tag{24}$$

Internal boundary point treatment method for drainage channel flow into paddy field

Consider the case where the water flow of a drainage channel enters into paddy field through the irrigation gate, as shown in Fig. 5.

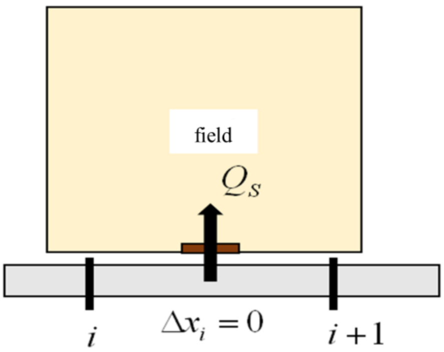

Fig. 5. When the water flow of drainage canal enters into paddy field

Then, to determine the backward-forward coefficients, we assume the following continuity condition:

$$\begin{cases} Z_i = Z_{i+1} = Z_s \\ Q_{i+1} = Q_i - Q_s \end{cases} \tag{25}$$

Where, Q_s is the inflow from the drainage channel to the paddy field (m^3/s).

Transforming Eq. (25) into

$$\begin{cases} Z_i^n + \Delta Z_i = Z_{i+1}^n + \Delta Z_{i+1} \\ Q_{i+1}^n + \Delta Q_{i+1} = Q_i^n + \Delta Q_i - Q_s \end{cases} \tag{26}$$

From the continuity equation in paddy field

$$Q_s = \frac{A_s\left(Z_i^n\right)}{\Delta t} \Delta Z_{i+1} \tag{27}$$

Substituting the relationship between Eq. (27) and $\Delta Q_i = F_i \Delta Z_i + G_i$ into Eq. (26) and ordering, the backward-forward coefficients are determined as follows:

$$\begin{cases} F_{i+1} = F_i - \frac{A_s\left(Z_i^n\right)}{\Delta t} \\ G_{i+1} = G_i + Q_i^n - Q_{i+1}^n \\ H_i = 0 \\ I_i = 1 \\ J_i = Z_{i+1}^n - Z_i^m \end{cases} \tag{28}$$

Drainage system simulation analysis process of paddy zone

Figures 6 and 7 show the different connection state of different paddy fields and drains. If hundreds of paddy fields and several drainages are combined to form a paddy zone, numerical calculations must be performed on the basis of the first set of cross-section calculation order of paddy fields and drainages to simulate the inflow and outflow processes, reflecting the combination of individual paddy fields and drainages.

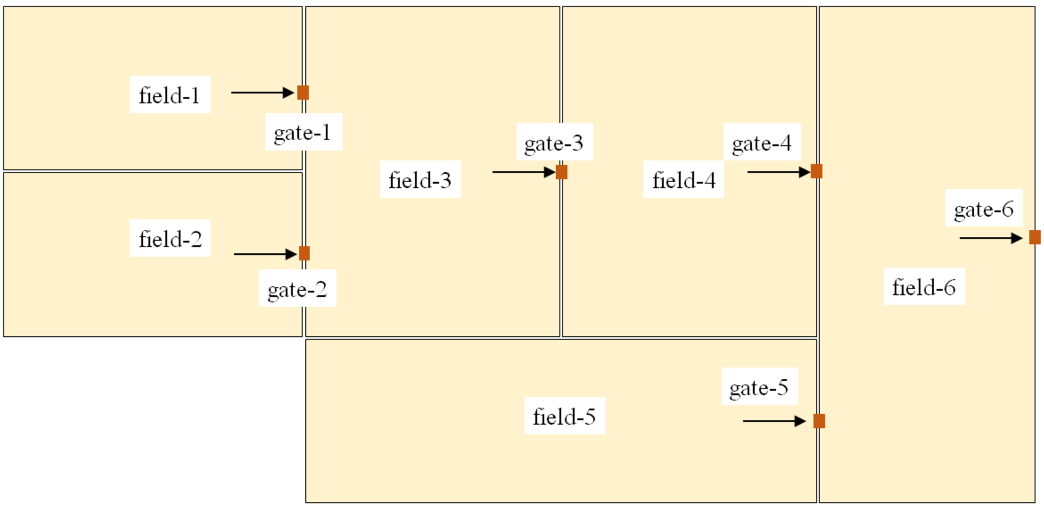

Fig. 6. Different connection states of paddy fields.

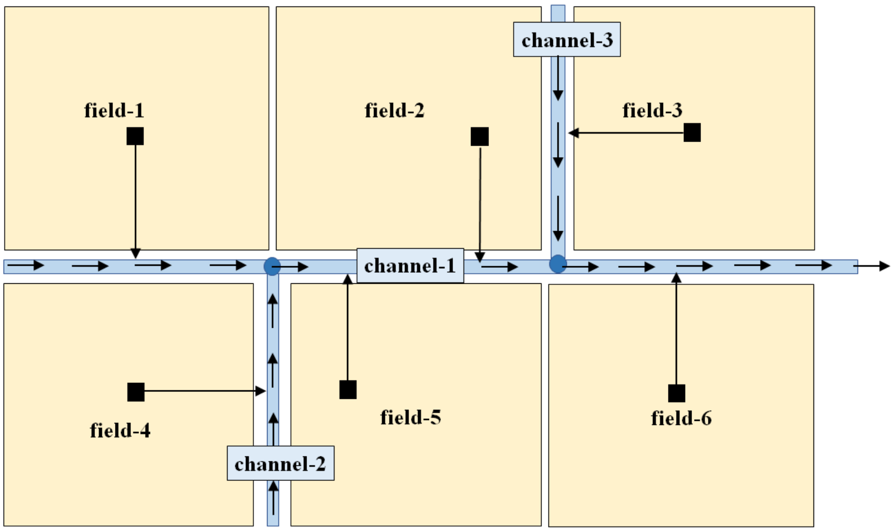

Fig. 7. Different connection states of drainages.

In this paper, a new numerical algorithm is proposed to perform the runoff simulation analysis while automatically searching for the paddy field calculation orders by analyzing the complex coupling relationships of these paddy fields.

Some of the paddy field class structures representing a paddy field are as follows:

Structure of paddy field class *field*(){

Integer *center_paddy_x*//*x* coordinate of paddy field center

Integer *center_paddy_y*//*y* coordinate of paddy field center

Integer *output_paddy_x* //*x* coordinate of paddy field outlet

Integer *output_paddy_y* //*y* coordinate of paddy field outlet

Integer *up_n** //number of influent paddy fields

Integer *up_no( )* //No of influent paddy field

Integer *dn_n* //number of discharged irrigation gates (paddy fields)

Integer *dn_no( )* //No of discharged paddy field

Integer *channel_n* //number of drainages connected to paddy field

...

}

Figure 8 shows a class of paddy fields represented by a diagram.

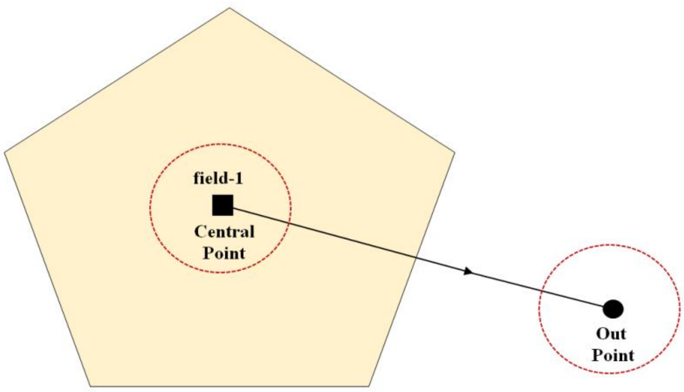

Fig. 8. Graphical representation of a paddy field class

The structure of the paddy field class includes, first, the attribute variables to store the number of paddy fields that are influenced into the paddy fields and the number of paddy fields that are discharged from the paddy fields. Next, there are central point storage variables and output point storage variables that characterize the location and discharge direction of the paddy field.

There are many cross sections in a single drain and, in order to ensure the stability of the numerical solution, there must be more than one non-junction section between the sections where the drainage channel and paddy field (irrigation gate) are combined. For example, if paddy fields of 50m width are connected to a drainage channel, there should be four ~ five sections per 50m to be placed more than one drainage section between the sections where paddy fields in the left and right sides of the drainage channel are joined. Therefore, it is reasonable to set one section per 10 ~ 15m in the drainage channel.

Some of the single drainage channel class structures are as follows.

Structure of the drainage channel class *channel* () {

Integer *level* //grade of drainage channel

Integer *cross_n* //number of cross-sections

Integer *cross_x*() //*x* coordinate of cross section

Integer *cross_y*() //*y* coordinate of cross section

Integer *cross_index*() //calculation number of cross section

Integer *paddy_no*() //paddy field number connected to the cross section

...

}

The structure of the drainage channel class includes the attribute variables to store the number, the location and the calculation rank of sections of the corresponding drainage channel.

① Set the initial and simulation conditions of the calculations.

Input the rainfall time series in the paddy field and set the calculation initial water levels (drainage channel water level and water level of individual paddy fields).

Set the calculation time interval (usually 5s) and simulation time.

The paddy field area and the width, the height and the flow coefficients of irrigation gate for individual paddy fields are set.

Input the upstream and downstream boundary conditions, bed roughness coefficient, cross-sectional view, and initial flow rate for the individual drainage channel sections of the paddy zone.

② Identify the connection state of paddy fields and drainage channel sections in the paddy zone.

The connection state of paddy fields is stored in the corresponding storage variables, comparing the central and output points of individual paddy fields. Based on the values of these storage variables, the corresponding values are also stored in the storage variables that reflect the inflow and outflow relationships between paddy fields, paddy fields and drainage channels.

Comparing the locations of individual drainage sections, the connection state of drainage channel sections is stored in the corresponding storage variables.

③ Search for paddy field calculation rank.

The simulation of the runoff in the paddy zone should be carried out one by one from the paddy field farthest from the drainage channel. For this, the paddy field, which is the most distant from the drainage channel, should be searched and the calculation rank of the paddy fields should be assigned.

For automatic search of these paddy field computational ranks, a hierarchical search rule was established.

The layers were divided into upper, middle and lower boundary layers, and the computational ranks were assigned to the paddy fields entering the corresponding layer.

The process of assigning the detailed computational ranks is as follows.

First, we establish the initial computational ranks based on the values of the attribute variables *up_n*, *dn_n*, and *channel_n* of the paddy field class.

First, in the case of *up_n*=0, *dn_n*≥1, and *channel_n*=0, these paddy fields haven't the influent paddy fields and only have the discharged irrigation gates so these paddy fields belong to the upper boundary layer. Assuming the number of these paddy fields to be *n*, we assign a unique rank from 1 to *n* to paddy fields.

Then, in the case of *up_n*≥1, *dn_n*≥1, and *channel_n*=0, these paddy fields lie between paddy fields of the upper boundary layer and paddy fields connected to the drainage channel, i.e., these paddy fields belong to the middle layer. If the number of these paddy fields is *m*, the computation ranks should be assigned to paddy fields, starting from paddy fields directly connected to paddy fields of the upper boundary layer, from $n+1$ to $n+m$.

In the case of *up_n*≥1, *dn_n*=0, *channel_n*=1, these paddy fields are directly connected to the drainage channel and belong to the lower boundary layer. Assuming the number of these paddy fields is *p*, the computation ranks from $n+m+1$ to $n+m+p$ are assigned to these paddy fields.

If the set of paddy fields of the middle layer consists of several paddy fields connected in parallel, these paddy fields should be further divided into upper, middle and lower boundary layers and the computation ranks should be reassigned from $n+1$ to $n+m$.

In this case, paddy fields directly connected to the initial upper boundary layer are searched for paddy fields of the upper boundary layer in the second stage, paddy fields directly connected to the initial lower boundary layer are searched for paddy fields of the lower boundary layer in the second stage, and paddy fields lying between them are included in the middle layer in the second stage.

This process is repeated until there is no case of paddy fields connecting in parallel the middle layer.

④ Search for the drainage channel section computation rank.

In the drainage channel system, the main drainage and branch drainage are classified.

In case the final section location of the individual drainage channel does not coincide with any non-final section location of other drainage channel, we set this drainage channel as the main drainage and assign a value of 0 to the attribute variable *level*.

Then, in case the final section location of the individual drainage channel coincides with any section location of main drainage channel, the first-grade branch drainage is determined and the value of *level* is set to 1.

In case the final section location of the individual drainage channel coincides with any section location of first-grade drainage channel, second-grade branch drainage is determined and the value of *level* is set to 2. In this way, the drainage system is classified into main and branch drainage channels at all grades.

As a next step, the computation ranks are assigned to the cross sections of the main and branch drains.

Number 1 is assigned to the starting section of the main drain. Then, starting from the starting section, we compare the *cross_x*, *cross_y* values of the individual sections with those of all sections of the other drainage channels, and unique rank to the corresponding sections are assigned until the values are not equal. If the number of such sections is *P*, then computation ranks are assigned from 2 to $P+1$ to these sections.

If the value is the same, this section is considered as the first confluence point, the computation rank of the starting section of the connected branch drainage channel is set to $P+2$, and unique ranks are assigned from $P+3$ to the cross sections to the confluent position.

Then, again comparing the location of cross sections from first confluence point, the second confluence point is searched and the computation ranks are assigned in the same way as above. In this way, confluence points search and computation ranking are performed to the final section of the main drainage.

If the computation ranking of the drainage system has finished, the computation ranks of drainage channel sections in which the paddy field is connected are stored in the attribute variable *paddy_n*, starting from the starting section.

The assigned computation ranks of the drainage sections are shown in the figure as follows:

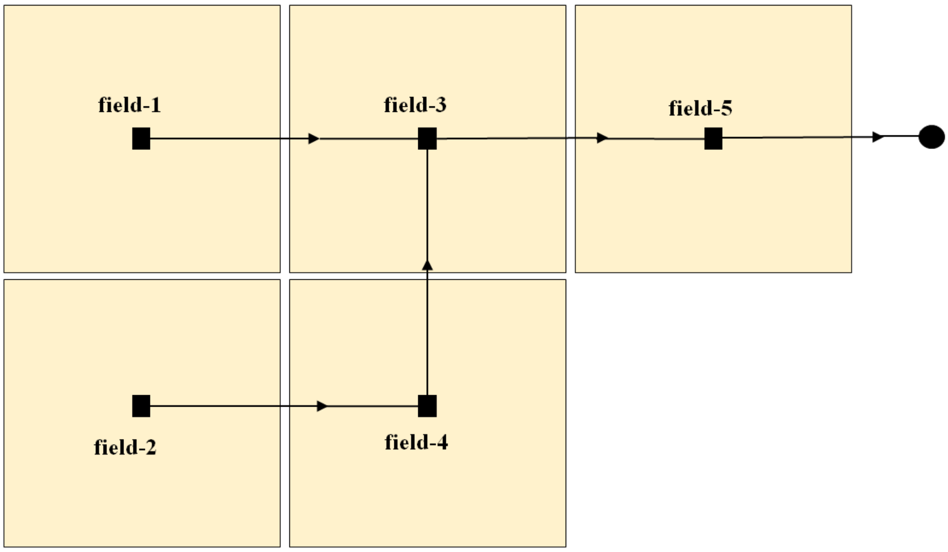

Fig. 9. Connection state representation of paddy fields using paddy field class

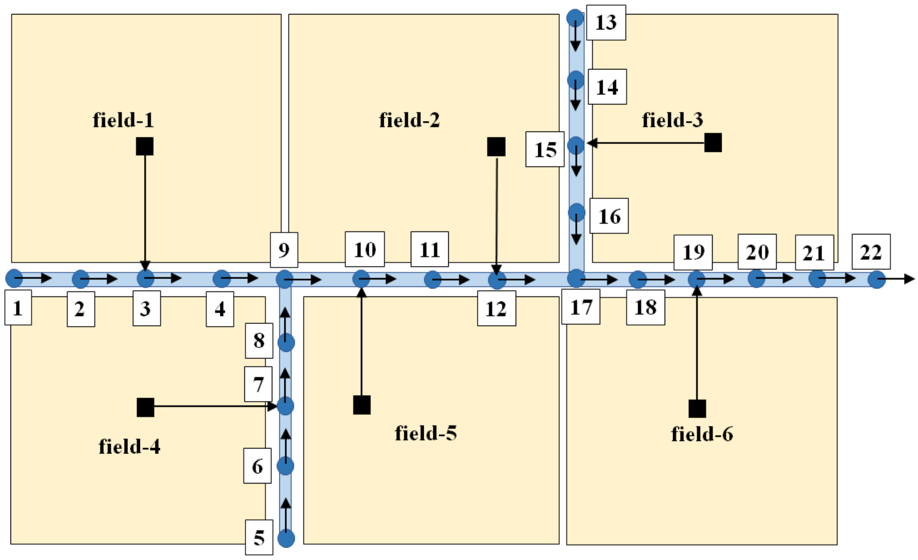

Fig.10. Computation rank search of drainage channel section

⑤ The runoff calculation of paddy zone should be performed.

According to computation ranks determined in Step 3, the runoff calculation through the irrigation gate of individual paddy fields is performed.

If the irrigation gate is not flooded, Eq. (9) and if the irrigation gate is flooded, Eq. (10) are used to calculate from paddy fields in the upper layer to paddy fields in lower layer. At that time, the calculation is repeated until the calculated values coincide with the assuming water depth above the irrigation gate at the corresponding calculation time by applying an iteration method in individual paddy fields.

According to the drainage channel section computation ranks determined in Step 4, the forward coefficients F_i and G_i in the individual drainage sections are determined and according to the set upper and lower boundary conditions, the water height and flow rate of the drainage sections are calculated. The backward-forward coefficients are determined by comparing the water level of the drainage channel and the paddy field irrigation gate in the cross-sections connected to the paddy field using Eqs. (23) and (27).

Increasing the calculation time, the water level and flow rate in each paddy field and drainage channel section are calculated.

Results and discussion

Placement and connection of element objects for the drainage system simulation analysis of the Suk Hwa tideland

Figure 11 shows a map of some catchments, paddy fields, drainage channels and regulating pond of Suk Hwa tideland in Sonchon County, East Phyongan Province of the DPRK, by using the newly developed tideland drainage simulation system.

Fig.11. Drawing of connection state between paddy fields, drainage channels, regulating ponds and drainage gates.

Three catchments, 176 paddy fields, four branch drainage channels and one regulating pond connected to the sea through drainage gates.

Currently, three catchments are directly connected to the sea through a river channel. However, in this case, the high tide causes the rise of sea water along the river channel to negatively affect the channel capacity, and furthermore, the risk of flooding the reclaimed tideland paddy zone in the case of the overlap of tides with the flood discharge formed in the catchment during the flood period is high.

In this context, a drainage scheme was proposed to concentrate all the inflows in the reclaimed tideland paddy zone and the inflows of the channeling ditches connecting the three catchments, to organize discharge as much as possible during the low tide period, and to adjust by using the available volume of regulating pond during the high tide period, and a drainage system simulation analysis was carried out to determine the number of drainage gates to use effectively the available volume of regulating pond.

Figures 12, 13, 14 and 15 show the details of the connection state of each component of the drainage system.

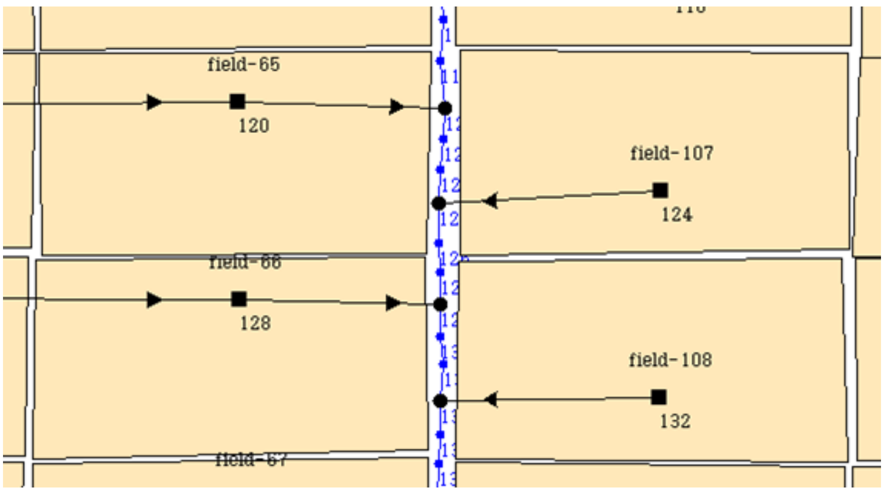

Fig. 12. Connection state between paddy fields, paddy field and drainage channel as shown in the expansion.

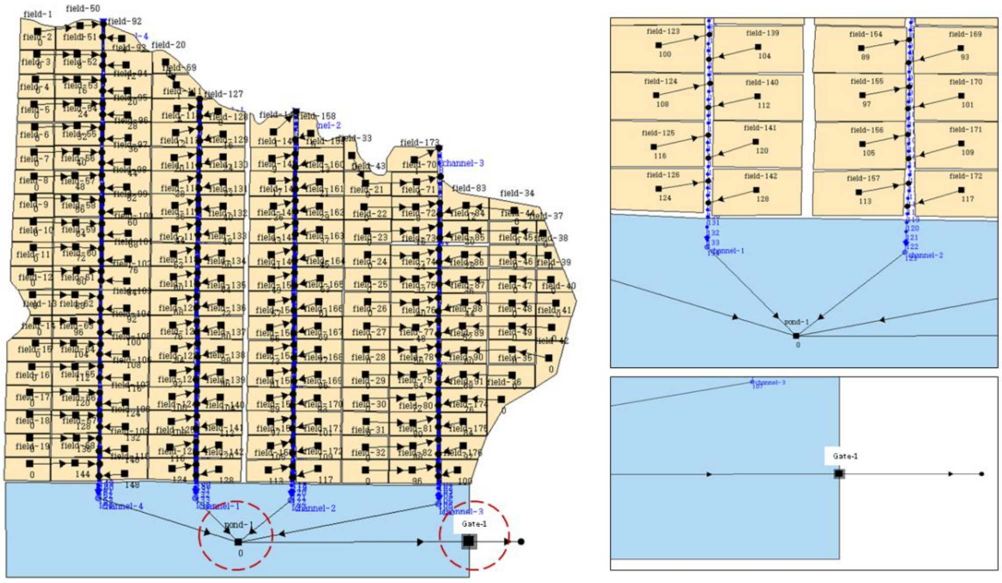

Fig.13. Connection state of the drainage channel and regulating pond and drainage gates as shown in the expansion

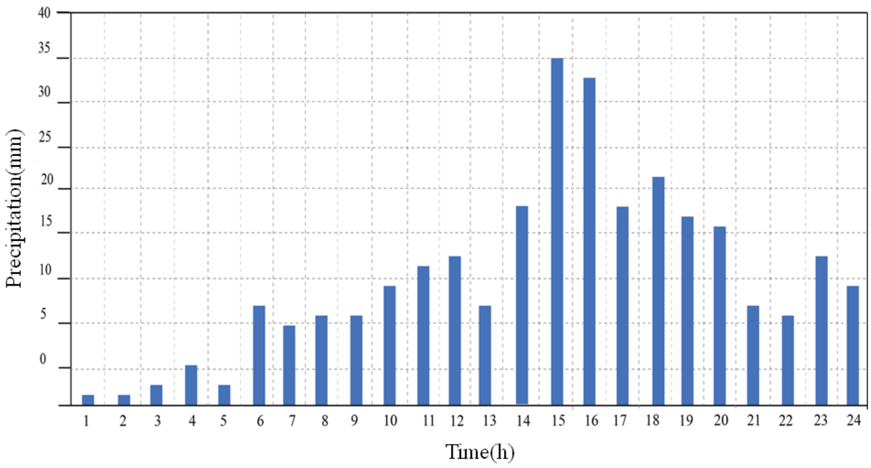

Fig. 14. Precipitation process from July 11 to July 12, 2023

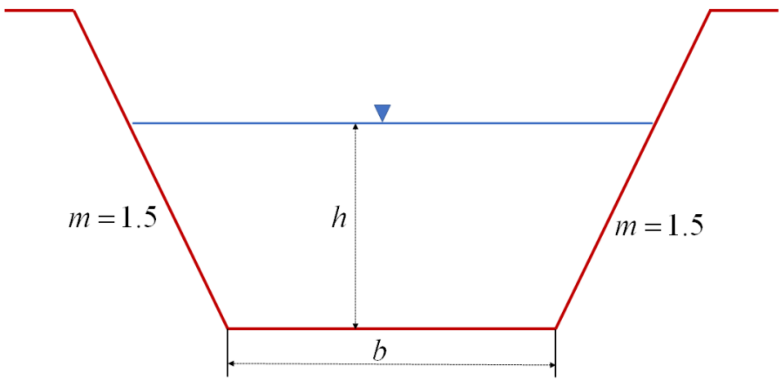

Fig.15. Drainage channel cross-section

Accuracy assessment of the drainage system simulation analysis method of tideland paddy zone

To verify the accuracy of the proposed drainage system simulation analysis method, a comparative analysis was first carried out between the data observed during the flood period in July 2023 and the values simulated reproducing the situation.

The number of paddy fields is 176 and the total area is 84.8 hectares. Figure 14 shows the hourly precipitation distribution over 24 hours between July 11 and July 12, 2023.

The channel section of the drainage is shown in Fig. 15.

Where, b=1.5m and h=1.0m.

The simulation conditions for individual paddy fields are set as Table 1.

Table 1 Parameter settings for the runoff calculation of paddy fields

No	Runoff co efficient	Irrigation ga te width(m)	Irrigation ga te height (m)	Paddy field ar ea (m^2)	Bottom he ight (m)	Initial water level(m)
1	0.67	0.5	3.04	1 476	3.24	3.24
2	0.67	0.5	3.02	1 271	3.22	3.22
3	0.67	0.5	2.99	1 316	3.19	3.19
4	0.67	0.5	2.84	1 436	3.04	3.04
5	0.67	0.5	2.78	1 240	2.98	2.98
6	0.67	0.5	2.7	1 391	2.9	2.9
7	0.67	0.5	2.65	1 413	2.85	2.85
…	…	…	…	…	…	…
173	0.67	0.5	2.24	1 634	2.44	2.44
174	0.67	0.5	1.57	1 633	1.77	1.77
175	0.67	0.5	1.47	1 597	1.67	1.67
176	0.67	0.5	1.36	1 360	1.56	1.56

As shown in Fig. 11, the main drainage channel has four drainage channels, 117 computational cross-sections of the first-degree drainage channel, 101 computational cross-sections of the second-degree drainage channel, 93 computational cross-sections of the third-degree drainage channel, 85 computational cross-sections of the fourth-degree drainage channel, and the distance between the computational sections is set to 10 m.

Table 2 shows the set of channel simulation conditions for the drainage system.

Table 2 Parameter settings for water flow numerical calculation of drainage channels

No	Number of cross-sections	Cross-sectional distance(m)	Roughness coefficient
1	117	10	0.031
2	101	10	0.031
3	93	10	0.031
4	85	10	0.031

The total calculation time was set to 72h and the calculation time interval was set to 5s.

The height-area data of the regulation pond are shown in Table 3 and the initial water level is 1.0m.

Table 3 Height-area data of regulation pond

HEIGHT (M)	-1.9	-1.4	-0.9	-0.4	0.0	0.1	0.6	1.1	1.6	2.1
AREA (HECTARE)	0	2	46	100	145	155	225	294	384	473

The simulation conditions of the drainage gate are set as shown in Table 4.

Table 4. Characterization of the drain gate

Width (m)	Height (m)	Sill height (m)	Number of drainage gate opened (unit)
1.0	1.0	-0.8	2

Fig. 16 shows the locations of the water gauges and flow meters located in paddy fields and drainage channels.

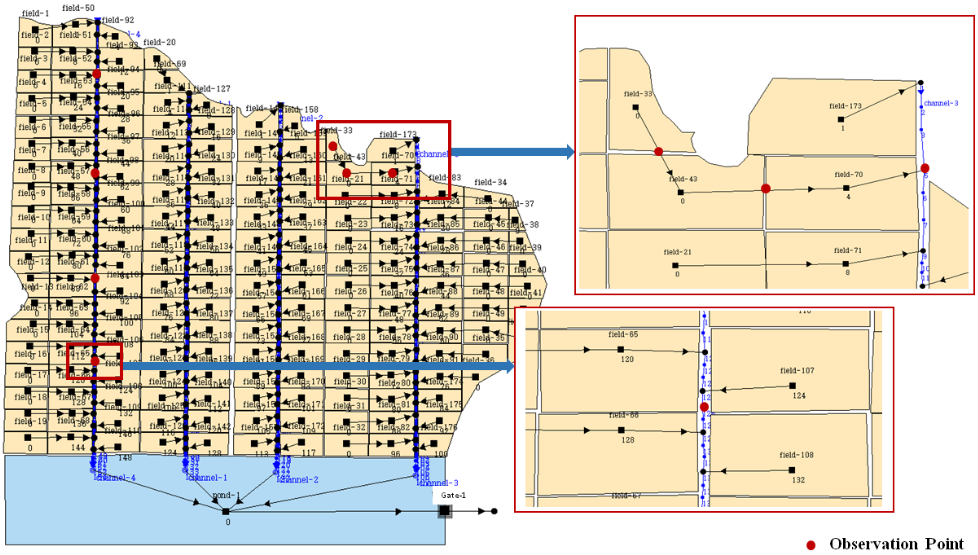

Fig. 16. Layout of observation points

As shown in the figure, four water gauges are installed in drain-1 and three flow meters are installed in paddy field irrigation gates.

Fig. 17 shows the comparison results between the discharge observed from 11 to 12 July 2012 and the discharge calculated using the paddy field runoff simulation method presented in this paper.

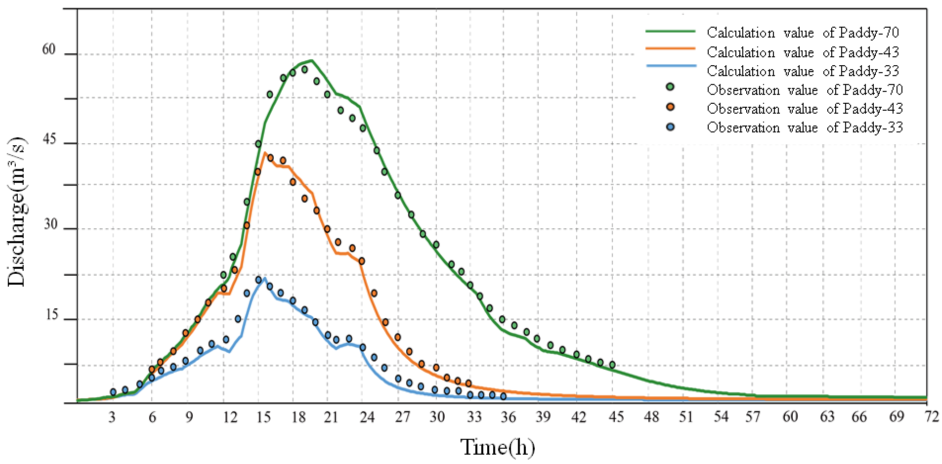

Fig. 17. Comparison of discharge in individual paddy field irrigation gates

The comparison between the observed and calculated values in drain-1 is shown in Fig. 18.

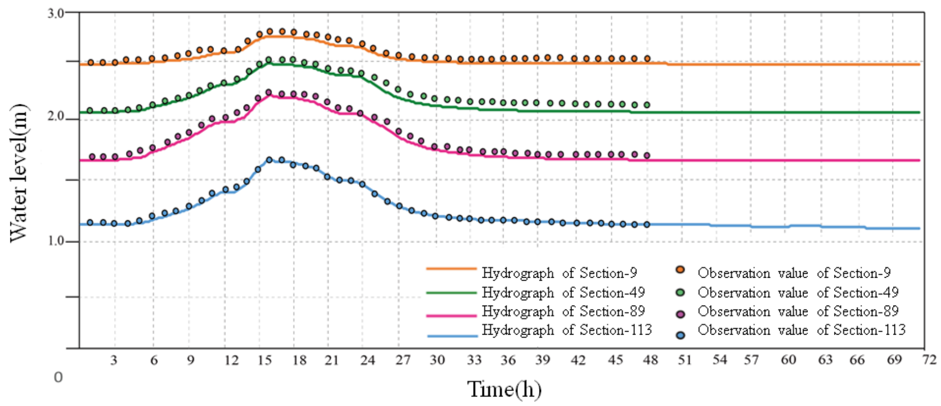

Fig. 18. Comparison of water level processes in the calculation sections of drain-1.

As can be seen from the figures, the calculated irrigation gate discharge and hydrograph at the observation points of the drainage channel and paddy fields coincide very well with the observations. The average relative error is % in the case of the irrigation gate discharge, and is % in the case of hydrograph. Hence, the proposed method can be applied to the real problem with sufficient accuracy.

Drainage gate number determination of regulation pond in the presence of inflow of a channeling ditch

In this paper, based on the accuracy of the simulation analysis of drainage systems in paddy zone, a simulation calculation was carried out to determine the number of drainage gates in the regulation ponds for 100-year period flood events.

The initial level of regulation pond was set to 1.18m, the maximum permissible level was set to 1.3m, and the final level of regulation to be lowered after 72h was set to 0.5m.

Fig. 19 shows the hourly precipitation distribution for 308mm of 24h maximum rainfall.

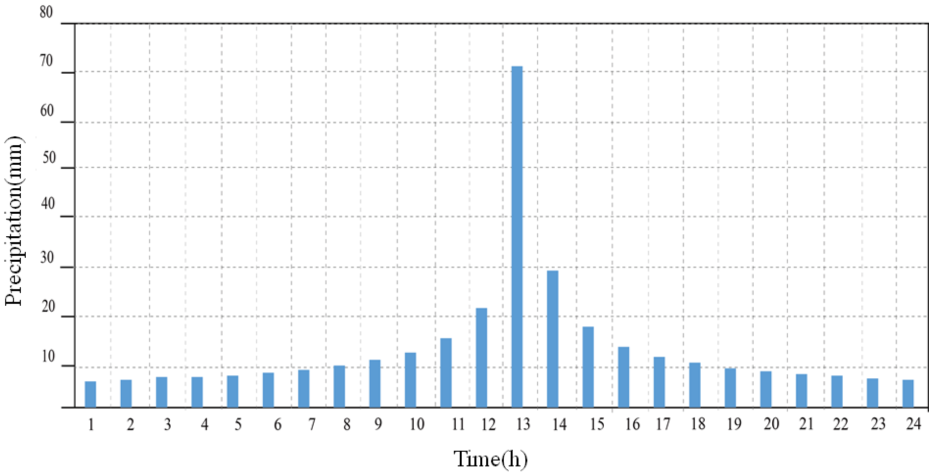

Figure.19. 24 Hourly distribution of 24 h maximum rainfall

Fig. 20 shows the detailed connection state between the individual elements of the drainage system, assuming that the channeling ditch enters a regulation pond.

Fig.20. Connection state between catchment, channeling ditch, paddy field, drainage channel, regulation pond and drainage gate

As can be seen from the figures, the flood inflow formed in catchment-1, catchment-2 and catchment-3 due to the 24-h maximum rainfall is flowing into the regulation pond through two river channels. The maximum value of flood pr ㅎ쥬ㄷ ocesses flowing through the river channel connected to the catchment-1 is 25.6m3/s, and the maximum value of flood processes flowing through the river channel connected to the catchment-2 and catchment-3 is 37.8m3/s.

The maximum value of the inflow process that flows into the regulation pond through paddy zone drainage channels is 8.32m3/s.

Under such conditions, simulations were carried out to determine the size and number of drainage gates under conditions that do not change the volume of the regulation pond.

Fig. 23 shows the results of the runoff control calculations for the regulation pond with the number of gates in the case of a 2m×2m gate.

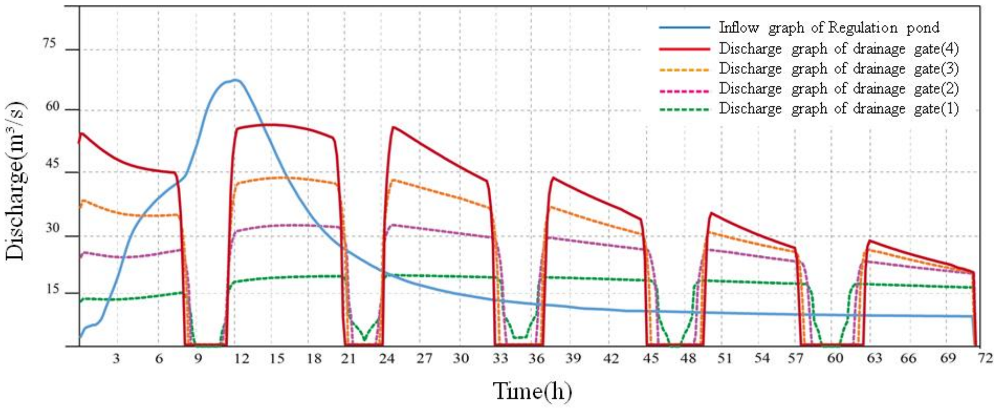

Fig.23. Calculation results of the runoff control in the regulation pond.

The maximum peak flow of flood inflow process in the paddy field and river channels that flow into the regulation pond is 66.9m3/s.

In the figure, when the sea level is above the internal level of the regulation pond, the discharge is stopped and the gate is opened during the low tide to achieve a concentrated discharge. With the increase of the number of gates, the discharge during the low tide also increases. It can be seen that the difference of the discharge change amplitude with the number of gates at individual low tide periods are due to the difference of discharge capacity of the drainage gate with the water level of the regulation pond, and the higher the water level, the larger the discharge change amplitude.

Fig. 24 shows the hydrograph of the water level change in the regulation pond, and Table 5 shows the maximum water level at the regulation pond with the number of gates and the final water level values after 72h.

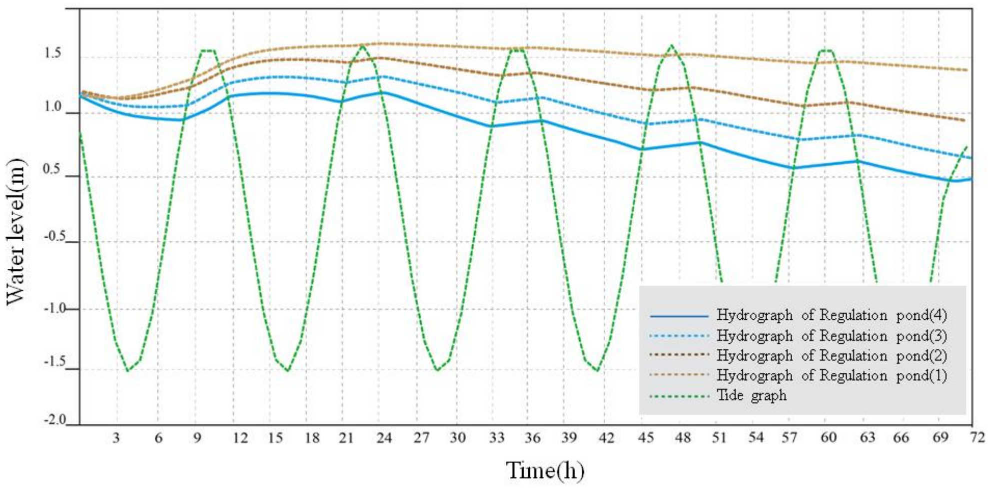

Fig.24. Hydrograph of water level change in regulation pond.

Table 5. Variation of maximum and final water levels in regulation pond with the number of drainage gate.

Number of drainage gate (unit)	Maximum water level (m)	Final water level (m)

1	1.65	1.41
2	1.45	0.92
3	1.28	0.69
4	1.13	0.50

As shown in Table 5, in the case of one or two gates, the maximum and final water levels do not satisfy the maximum permissible water level in the regulation pond and the final target water level.

In the case of three gates, the maximum level is below 1.4m, but the final water level is 0.69 m, exceeding 0.5 m. In the case of four gates, both the maximum and final water levels satisfy the simulation conditions.

To control the 100-year period flood that occur in the catchment and paddy zone around tideland, using the volume of existing regulating pond, four gates of at least 2m×2m size should be installed.

Conclusions

In this study, a new simulation analysis method of drainage system in tideland paddy zone was proposed by combining the runoff simulation analysis method of tideland paddy fields through irrigation gate and the water flow simulation analysis method of drainage channel system, and applied to the Suk Hwa tideland located in North Phyongan Province of the DPRK and verified its effectiveness.

First, a new runoff simulation analysis method of paddy zone combined with a search algorithm to determine the runoff computation ranks of paddy fields, reflecting the different combinations of paddy fields, is proposed.

Also, a method of determining the backward-forward coefficient for internal boundary treatment at the location where the main flow of the drainage channel and the paddy field irrigation gate flow are confluent was proposed and applied to the numerical calculation of the water flow in the drainage system.

The simulation analysis method of drainage system in tideland paddy zone, which combines the runoff simulation analysis method of paddy zone and the water flow numerical calculation method of drainage channel system, can be used effectively to verify the flood drainage capacity of tideland drainage system, to support the design of drainage system, and to determine the suitable location and scale of regulation pond for the prevention of flooding in the tideland paddy zone directly affected by tide.

Statements and Declarations

Data availability All data generated or analyzed during this study are included in this published article.

Authors' contributions Conceptualization: Yong-Gun Kim, methodology: Tong-Ho Ri and Ji-Song Choe, data collection: Kyong-Chol Pak and Hyon-Min Rim, analysis and investigation: Yong-Gun Kim and Tong-Ho Ri, writing of original draft and preparation: Ji-Song Choe, writing of review and editing: Kyong-Chol Pak and Hyon-Min Rim

Funding This current study was supported by the Kim Il Sung University, including salaries, equipment, and supplies.

Compliance with ethical standards

Competing interests The authors declare that they have no competing interests.

Ethics approval and consent to participate Not applicable

Consent for publication Not applicable

Acknowledgments

This study was supported by Kim Il Sung University, Pyongyang, the Democratic People's Republic of Korea.

References

1. Addab. H, Bailey.T(2022) Simulating the effect of subsurface tile drainage on watershed salinity using SWAT. Agricultural Water Management, 1-10. https://doi.org/10.1016/j.agwat.2021.107431
2. Afrasiabikia P, Rizi AP, Javan M(2017) Scenarios for improvement of water distribution in Doroodzan irrigation network based on hydraulic simulation. Computers and Electronics in Agriculture, 135:312–320. http://dx.doi.org/10.1016/j.compag.2017.02.011
3. Beharry SL Gabriels D, Lobo D, Ramsewak D, Clarke RM(2021) Use of the SWAT model for estimating reservoir volume in the Upper Navet watershed in Trinidad. SN Applied Sciences, 3:1-13. https://doi.org/10.1007/s42452-021-04201-7
4. Carrivick JL(2006), Application of 2D hydrodynamic modelling to high-magnitude outburst floods: An example from Kverkfjoll, Iceland. Journal of Hydrology, 321(1-4):187–199. https://doi.org/10.1016/j.jhydrol.2005.07.042
5. Chen Y, Marek GW, Marek TH, Porter DO, Brauer DK(2022) Simulating the effects of agricultural production practices on water conservation and crop yields using an improved SWAT model in the Texas High Plains. USA. Agricultural Water Management, 244:1-12. https://doi.org/10.1016/j.agwat.2020.106574
6. Christou A, Aguera A, Bayona JM, Cytryn E, Fotopoulos V, Lambropoulou D, Manaia CM., Michael C, Revitt M, Schroder P(2017) The potential implications of reclaimed wastewater reuse for irrigation on the agricultural environment: the knowns and unknowns of the fate of antibiotics and antibiotic resistant bacteria and resistance genes – A review. Water Research, 128:1-80. https://doi.org/10.1016/j.watres.2017.07.004
7. Dau QV, Kuntiyawichai K, Plermkamon V(2017) Quantification of flood damage under potential climate change impacts in central Vietnam. Irrigation and drainage, 66: 842–853. http://dx.doi.org/10.1002/ird.2160
8. Gerlach RM, Ahmed I, Beckman ND, Karim A(2016) The utility of HEC-1 flood hydrograph package in distributed flow guided area drainage master plan discharges verification in a desert environment. J. Hydrology Science and Technology, 6(3), 199-225
9. Happonen M, Koivusalo H, Malve O, Perkola N, Juntunen J, Huttula T(2016) Contamination risk of raw drinking water caused by PFOA sources along a river reach in south-western Finland. Science of the Total Environment, 541:74–82. http://dx.doi.org/10.1016/j.scitotenv.2015.09.008
10. Harsha S.S, Agarwal S, Kiran CH(2020) Regional Flood Forecasting using SWMM for Urban Catchment. International Journal of Engineering and Advanced Technology (IJEAT) 9(3):1027-1031. https://doi.org/10.35940/ijeat.C4798.029320
11. Hoghooghi1 N(2021) Assessing hydrologic and water quality effects of land use conversion to Brassica carinata as a winter biofuel crop in the southeastern coastal plain of Georgia, USA using the SWAT model. GCB Bioenergy, 13:473–492. http://doi.org 10.1111/gcbb.12792
12. Jiang L, Chen YB, Wang HY(2015) Urban flood simulation based on the SWMM model, Remote Sensing and GIS for Hydrology and Water Resources, 368:186-191. doi:10.5194/piahs-368-186-2015
13. Kim YG, Kim P, Jo MB, Oh SN, Paek CH (2019) A study on the one-dimensional flood numerical analysis method in open channels of Cascade barrage network. J Test Eval 49(1):20180959. https://doi.org/10.1520 /JTE20180959
14. KhornN, Ismail MH, Nurhidayu S, Kamarudin N, Sulaiman MS(2022) Land use/land cover changes and its impact on runoff using SWAT model in the upper Prek Thnot watershed in Cambodia. Environmental Earth Sciences, 81:1-14. https://doi.org/10.1007/s12665-022-10583-7
15. Khodashenas SR, Tajbakhsh M(2016) Management of Urban Drainage System Using Integrated MIKE SWMM and GIS. Journal of Water Resource and Hydraulic Engineering. 5(1)36-45. https://doi.org/10.5963/JWRHE0501004
16. Nasiri S, Ansari H, Ziaei AN (2020) Simulation of water balance equation components using SWAT model in Samalqan Watershed (Iran). Arabian Journal of Geosciences. 13(11):1-15. https://doi.org/10.1007/s12517-020-05366-y
17. Ontowirjo B, Fathurrahman I, Ramadhan M V, Zahriani A, Zahra M, Wahyudi H.(2023) LiDAR DEM and HEC-RAS On-Grid Rainfall Hydrograph Model for Irrigation System. IOP Conference Series: Earth and Environmental Science. 1198:1-7. https://doi.org/10.1088/1755-1315/1198/1/012023

18. Patra JP,Kumar R, Mani P(2016) Combined fluvial and pluvial flood inundation modelling for a project site. Procedia Technology, 24:93–100. http://creativecommons.org/licenses/by-nc-nd/4.0

19. Pachaly RL, Vasconcelos JG, Allasia DG, Tassi R, Bocchi JP (2020) Comparing SWMM 5.1 Calculation Alternatives to Represent Unsteady Stormwater Sewer Flows. Journal of Hydraulic Engineering, April. 146(7):1-16. https://doi.org/10.1061/(ASCE)HY.1943-7900.0001762

20. Perin R, Trigatti M, Nicolini M, Campolo M, Goi D(2020) Automated calibration of the EPA-SWMM model for a small suburban catchment using PEST: a case study. Environ Monit Assess, May. 192(6):1-17. https://doi.org/10.1007/s10661-020-08338-7

21. Rahman MM, Lin Z, Jia X, Streele DD, Desutter TM(2014) Impact of subsurface drainage on streamflows in the Red River of the North basin. Journal of Hydrology, 511:474–483. http://dx.doi.org/10.1016/j.jhydrol.2014.01.070

22. Rujner H, Leonhardt G, Marsalek J, Viklander M(2018) High-resolution modelling of the grass swale response to runoff inflows with Mike SHE. Journal of Hydrology, 562:411-422. https://doi.org/10.1016/j.jhydrol.2018.05.024

23. Roy B, Khan SM, Islam A.K.M.S, Mohammed K, Khan JU(2021) Climate‑induced flood inundation for the Arial Khan River of Bangladesh using open‑source SWAT and HEC‑RAS model for RCP8.5‑SSP5 scenario. SN Applied Sciences, 3:1-13https://doi.org/10.1007/s42452-021-04460-4

24. Tu M, Wadzuk B, Traver R(2020), Methodology to simulate unsaturated zone hydrology in Storm Water Management Model (SWMM) for green infrastructure design and evaluation. PLOS ONE, 15(7):1-19. https://doi.org/10.1371/journal.pone.0235528

25. Tarekegn TH, Haile AT, Rientjes T, Reggiani P, Alkema D(2010) Assessment of an ASTER-generated DEM for 2D hydrodynamic flood modeling. International Journal of Applied Earth Observation and Geoinformation, 12(6):457–465. https://doi.org/10.1016/j.jag.2010.05.007

26. Xie Z, Chen S, Huang J, Li D Lu X(2023) Patterns and drivers of fecal coliform exports in a typhoon-affected watershed: insights from 10-year observations and SWAT model. Journal of Cleaner Production, 406:1-11. https://doi.org/10.1016/j.jclepro.2023.137044